Spectroscopic, Kinetic, and Structural Properties of Rotamers of the 2-Vinylpyridinium Ylide of Phenylchlorocarbene

Roland Bonneau,*,† Daniel Collado,†,‡ Michel Dalibart,† and Michael T. H. Liu†,§

UMR 5803, CNRS & Université Bordeaux 1, 33405 Talence Cedex, France

Received: August 19, 2003; In Final Form: November 10, 2003

The analysis of the time-resolved UV−vis absorption spectra of the 2-vinylpyridinium ylide of phenylchlorocarbene, measured by laser-flash photolysis, indicates the existence of two rotamers of this species. The absorption spectrum, rise time, and decay time of each rotamer were determined by a global analysis method. The kinetic analysis of the results indicates an interconversion between the rotamers and a large difference between their rates of cyclization. The observed rotamerism involves a rotation of the vinyl pyridine with respect to the carbene, the two rotamers being differentiated by the fact that the vinyl group faces either the chlorine or the phenyl groups of the carbene. Calculations of the absorption spectra and enthalpies of formation of numerous possible structures indicate that the 100-nm difference between the wavelengths of maximum absorption is well explained by a change in the tilt angle between the phenyl and the ylide planes from 35−40° for the "red-absorbing" ylide to 55−60° for the other. However, the calculated enthalpies of formation of the various structures being nearly the same, these calculations do not allow us to assign one specific structure to one or the other of the observed species.

Introduction

Rotamers are isomers obtained by rotation around a single bond linking the two parts of a molecular structure when (i) these two parts are nonsymmetric with respect to the axis of this bond and (ii) the structure is stabilized for some specific values of the rotation angle. In some cases, the rotameric species can be isolated and their reactivities may be compared,[1] but rotamers are usually in fast equilibrium. Numerous spectroscopic studies have been made to extract the individual photophysical and photochemical properties of each rotamer from measurements on their mixture.[2]

The intermediate species **X** involved in stepwise cycloaddition reactions, $\mathbf{A} + \mathbf{B} \rightarrow \mathbf{X} \rightarrow \mathbf{C}$, where **X** stands for $\mathbf{A}^{\bullet}-\mathbf{B}^{\bullet}$ or $\mathbf{A}^{+}-\mathbf{B}^{-}$, should exist as rotamers when **A** and **B** are nonsymmetric with respect to the axis of the **A**−**B** bond, each rotamer corresponding to a specific orientation of the reactants during the formation of this bond. Sometimes the existence of rotameric forms of **X** can be deduced from the formation of stereoisomers of **C**, but there are very few examples of the direct observation of the **X** rotamers by time-resolved spectroscopy.[3] Yet, this approach offers information on the effect of geometric and steric factors on the rate constants of the reactions $\mathbf{A} + \mathbf{B} \rightarrow \mathbf{X}$ and $\mathbf{X} \rightarrow \mathbf{C}$ as well as on the possible equilibration between the **X** rotamers during their short lives.

Here we report the observation of two rotamers of the ylide resulting from the reaction between phenylchlorocarbene (**PCC**) and 2-vinylpyridine (**VP**), which, as shown some years ago,[4] rearranges to give a phenylindolizine after the elimination of HCl according to Scheme 1.

SCHEME 1

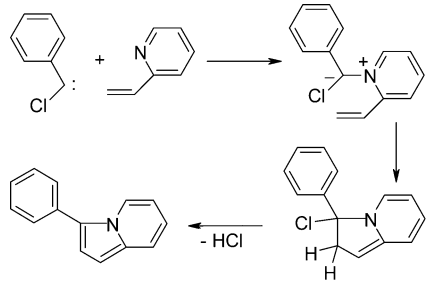

Experimental Section

Phenylchlorocarbene was generated by the photolysis of phenylchlorodiazirine in isooctane solvent by laser pulses at 355 nm. We prepared phenylchlorodiazirine from benzamidine by oxidation with NaOCl, according to the Graham procedure,[5] and purified it by chromatography on a silica column with *n*-hexane as the eluent.

The laser-flash-photolysis system uses a mode-locked Nd:YAG laser (Quantel), frequency-tripled, providing single pulses (200 ps, 20−30 mJ) at 355 nm as excitation. The 23-mm-diameter laser beam, with a Gaussian distribution of energy, passes through a 20-cm f.l. cylindrical lens so that the excitation beam is elliptic (23×6 mm^2) at the level of the sample cell. The central part of this ellipse is selected by a (10×3 mm^2) rectangular diaphragm to excite the sample in nearly homogeneous fashion. The light beam provided by a pulsed Osram XBO75 Xe arc passes through the excited part of the solution at a right angle to the laser beam and 0.5 mm behind the wall of the cell receiving the excitation, with a ($10 \times 2 \times 1.5$ mm^3) analysis volume. Because the effective optical path of the excitation is only 1.5 mm, the gradient of concentration of the transient species along the path of excitation is acceptable for solutions of diazirine with an absorbance at 355 nm of around 1 per cm. After passing through a monochromator, the transmit-

* Corresponding author. E-mail: r.bonneau@lpcm.u-bordeaux1.fr. Fax: +33 540 00 66 45.

† CNRS & Université Bordeaux.

‡ On leave from the Department of Organic Chemistry, University of Malaga, Spain.

§ Permanent address: University of Prince Edward Island, Charlottetown, P. E. I., Canada C1A 4P3.

10.1021/jp030991d CCC: $27.50
Published on Web 01/27/2004

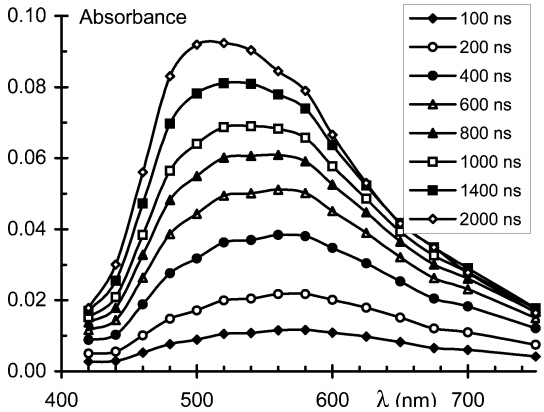

Figure 1. Transient absorption spectra recorded 0.1, 0.2, 0.4, 0.6, 0.8, 1.0, 1.4, and 2.0 μs after excitation.

ted light intensity is monitored by a Hamamatsu R 446 photomultiplier, and the electric signal is digitized and stored on a Tektronix TDS 620B digital oscilloscope (500 MHz, 2.5 GS/s). The time response of the detection system is less than 3 ns.

Geometries, heats of formation, and electronic absorption spectra were calculated using the software package CAChe 3.2 from Oxford Molecular Ltd. The input geometries are first refined by the molecular mechanics module using augmented MM2/MM3 parameters and then optimized by the MOPAC module with PM3 (or AM1) parameters, which also provides the heat of formation. The resulting geometry is finally used to calculate the UV absorption spectrum by ZINDO.

Results

Laser-Flash Photolysis. The transient absorption of the **PCC** carbene in the 310−315 nm range, produced by the excitation of solutions of phenylchlorodiazirine in isooctane, decays by a mixture of first- and second-order processes with a "lifetime" of a few microseconds. Upon the addition of **VP**, this decay becomes strictly first order, and the linear plot of the reciprocal lifetime versus [**VP**] yields a rate constant of ylide formation of around 1×10^8 M^{-1} s^{-1}. Simultaneously with the decay of the absorption of **PCC**, a broad absorption band with a maximum around 520 nm appears in the spectral range of 420−750 nm. This absorption, similar to that previously observed for the (***p*-Cl−PCC** + **VP**) ylide,[4] is assigned to the ylide **PCC←VP**. Compared to that of the **PCC**-pyridinium ylide,[6] the absorption spectrum of the ylide **PCC←VP** is red shifted by about 50 nm and shows a long "tail" on the red side (see Figure 1).

When it is monitored at 520 nm, this absorption grows according to approximately first-order kinetics, which depends linearly on [**VP**]. The pseudo-first-order rate constant for this growth is similar to, but significantly slower than, the rate constant for the decay of **PCC** under the same conditions (e.g., one obtains a 1.5-μs rise time at 520 nm when the decay time at 312 nm is only 1.1 μs). In addition, the rate of formation and the rate of decay of the ylide absorption depend on the wavelength of measurement. Both are noticeably slower in the central part than on the edges of the absorption band, as shown in Figure 2. The apparent lifetime is ~20 μs at 500 nm, whereas it is only ~7 μs at 750 nm. This clearly indicates that the observed transient absorption is due to several species.

We observed similar results in a study of the system (**VP** + *m*-phenylene-bis-chlorodiazirine).[7]

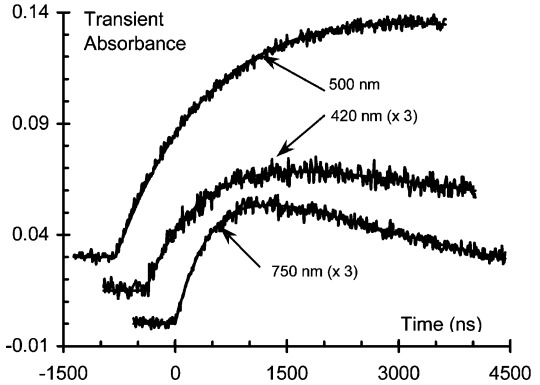

Figure 2. Experimental traces recorded at the same sweep rate at various observation wavelengths.

An inspection of the data reported by Naito et al.[8] reveals similar behavior for the 2-vinylpyridinium ylide of the (biphenyl-4-yl)chlorocarbene.

Deconvolution into Spectra of Two Species. Assuming that the transient absorption signal is due to only two different species with lifetimes of $\tau_1 \geq 20$ μs and $\tau_2 \leq 7$ μs, the absorption spectrum of the long-lived species is given by the transient absorption signal recorded 40 μs after excitation. The concentrations of the long- and short-lived species are respectively ≥13.5% (still measurable but "noisy") and ≤0.33% (negligible) of their initial values. Then, the absorption spectrum of the short-lived species may be estimated by subtracting from the transient absorption signal recorded a short time after excitation (e.g., 3 μs, close to the maximum) the contribution of the long-lived species (i.e., the transient absorption recorded 40 μs after excitation multiplied by a factor $\mathcal{F} = \exp[(t_1 - t_2)/\tau_1]$, with $t_1 = 40$ μs and $t_2 = 3$ μs in the present case). The value of $\mathcal{F}$ depends on the estimated τ_1 value and is refined to give a "nice" absorption spectrum of the short-lived species, a largely subjective criterion. In addition, this method gives noisy absorption spectra that need smoothing, which is a subjective operation, as well. This method gives absorption spectra with λ_{max} around 500 and 610 nm for the long- and short-lived species, respectively.

To avoid assumptions of the number of species and the subjective steps of the previous procedure, we analyzed the full set of absorption spectra recorded at various times after excitation by a factor analysis method.[9] First, a principal factor analysis (PFA) treatment of the matrix [absorbance vs (time, wavelength)] indicates that two species only, $\mathbf{Y_1}$ and $\mathbf{Y_2}$, are responsible for the transient absorption. Further transformation of the PFA solution by abstract factor analysis, involving mathematical rotations, finally gives the absorption spectrum and the time dependence of the concentration c of each of the two species shown in Figure 3a and b.

Then, as shown in Figure 3b, curve fitting of the values c_1 and $c_2 = f(t)$ by a function $c = c_0[\exp(-k_{dec}t) - \exp(-k_{gr}t)]$ yields the first-order rate constants for the growth (k_{gr}) and the decay (k_{dec}) of each species, given in Table 1. Let us emphasize that contrary to other transformation methods such as target factor analysis, which presupposes a well-defined shape function, or self-modeling methods, which impose known constraints, the abstract factor analysis does not request any a priori conditions.

The absorption spectra and time-dependence functions given by the factor analysis are normalized to 1 at their maximum because no assumption is made on the absorption coefficient values. To reproduce accurately the time-resolved spectra presented in Figure 1, the spectra shown in Figure 3a must be

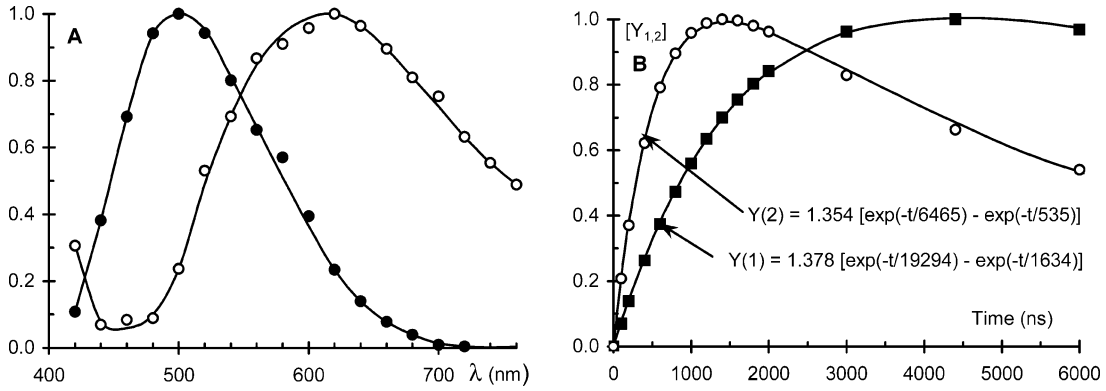

Figure 3. (A) Absorption spectra of the two species resulting from the global analysis of the data shown in Figure 1. (B) Time dependence of the concentration of the two species as given by the global analysis (points). The curves are drawn from the functions obtained by a nonlinear least-squares analysis of the data points.

TABLE 1: Spectroscopic and Kinetic Properties of Species Y_1 and Y_2 Resulting from the Global Analysis of the Time-Resolved Transient Absorption Data

species	λ_{max} (nm)	τ_{growth} (μs)	τ_{decay} (μs)
$\mathbf{Y_1}$	500	~1.6	~19
$\mathbf{Y_2}$	620	~0.53	~6.5

SCHEME 2

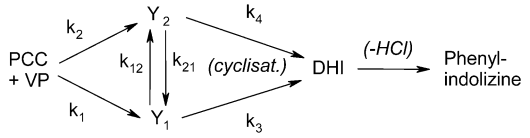

multiplied not only by their time-dependence function but also by a scaling coefficient that is 2.5 times lower for $\mathbf{Y_2}$ than for species $\mathbf{Y_1}$. This means that the maximum concentration of species $\mathbf{Y_2}$ multiplied by its absorption coefficient at 620 nm is 2.5 times lower than the maximum concentration of species $\mathbf{Y_1}$ multiplied by its absorption coefficient at 500 nm.

Discussion

Considering the similarity of their properties (absorption spectra, rates of formation, and rates of disappearance), species $\mathbf{Y_1}$ and $\mathbf{Y_2}$ must be similar and may be identified as rotameric forms of the ylide. Kinetically, the system may be represented by the mechanism shown in Scheme 2. Species $\mathbf{Y_1}$ and $\mathbf{Y_2}$ cannot be in fast equilibrium because their τ_{growth} and τ_{decay} differ by a factor of 3. By contrast, if there were no interconversion between them (i.e., if $k_{12} = k_{21} = 0$), then the growth of both species should follow pseudo-first-order kinetics (**VP** being in excess) with the same rate constant $k = (k_1 + k_2) \times [\mathbf{VP}]$.[10]

A numerical simulation of the time evolution of the system was made with the following parameters:

k_1 [**VP**] $= 8 \times 10^5$ s^{-1}, k_2 [**VP**] $= 6 \times 10^5$ s^{-1} (i.e., both rotamers are formed with similar rate constants[11,12]);

$k_{12} = 2 \times 10^4$ s^{-1} and $k_{21} = 2 \times 10^5$ s^{-1} (i.e., $\mathbf{Y_1}$ is slightly more stable than $\mathbf{Y_2}$, and the energy barrier between them is around 10 kcal/mol[13]);

$k_3 = 2 \times 10^4$ s^{-1} and $k_4 = 1 \times 10^5$ s^{-1} (i.e., the cyclization of $\mathbf{Y_2}$, the red-absorbing species, is a little bit easier than that of $\mathbf{Y_1}$).

The results are shown in Figure 4a. After normalization to their maxima, the time dependences of the concentration of rotamers given by this simulation nicely fit the time-dependence functions given by the factor analysis of the experimental data (Figure 3b). The concentrations reach their maximum values with about the same time values (~1.5 and 5.5 μs); the values of τ_{growth} determined as indicated in Figure 4b are similar to those given in Figure 3b; the ratio of the maximum concentrations ($\mathbf{Y_{1max}}/\mathbf{Y_{2max}}$) = 2.35 is close to the value of 2.5 found between the weights of the spectra shown in Figure 3a, as expected because the absorption coefficients of both rotamers are probably similar.

Even if the fit between experimental data and the results of a numerical simulation based on a postulated mechanism does not really demonstrate that this mechanism is correct, an interconversion between the two rotamers seems to be the only way to account for the differences between both of the τ_{growth} values and the absorption amplitudes of two species produced from a common precursor.

Structures of Rotamers. There are two possible rotamers for **VP** itself, α and β, and each one may give two rotameric

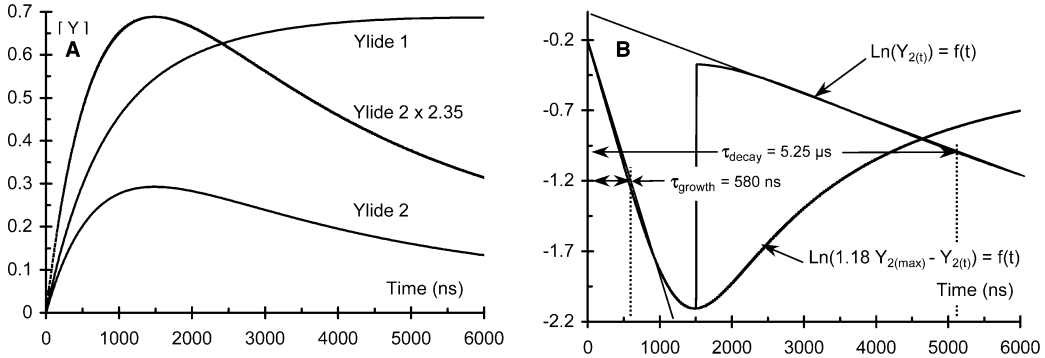

Figure 4. (A) Numerical simulation of the time dependence of the concentration of ylides $\mathbf{Y_1}$ and $\mathbf{Y_2}$ calculated on the basis of Scheme 3, with rate constant values given in the text. (B) Determination of τ_{growth} from the slope of the plot of ln[m A(max) − $A(t)$] vs time. The parameter m is adjusted to get a good linear fit of the part of the curve corresponding to the largest part of the growth. (It would be equal to 1.0 if the species were stable and is ~1.18 in this case.)

SCHEME 3

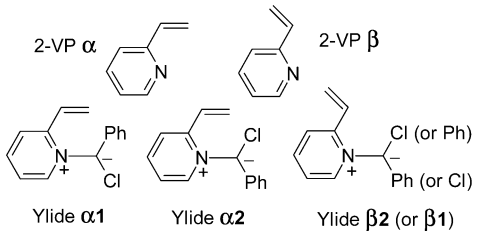

SCHEME 4

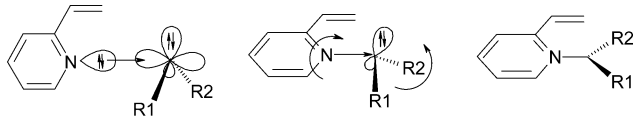

ylides with the vinyl group facing either the Cl atom, α**1** and *β***1**, or the phenyl, α**2** and *β***2**, as shown in Scheme 3.

Of course, the real ylide structures are not as planar as represented in Scheme 3. In fact, during the approach of **VP** by a singlet carbene, the molecular planes of these two species are perpendicular to maximize interactions between the nitrogen doublet and the empty $2p_\pi$ orbital. After or concomitant with the formation of the N−C bond, the pyridine then suffers a rotation around this new bond to maximize interactions between the electrons of the σ carbene orbital and the π pyridine orbitals, as shown in Scheme 4.

Depending on the orientation of this rotation, the vinyl group will face one or the other of the carbene substituents. The resulting structures possess many modes of deformation, such as the four rotations shown in Figure 5, and are far from planar: with respect to a planar structure, the values of the rotational angles predicted by calculations (see below) are in the following range of values: $30° < \theta < 60°$, $10° < \varphi < 30°$, and $35° < \omega < 65°$ for the α rotamers or $160° < \omega < 175°$ for the *β* rotamers.

Rotamerism α ↔ *β*. Molecular mechanics calculations predict the α rotamer of **VP** to be 4−5 kcal/mol more stable than the *β* rotamer. However, according to semiempirical quantum mechanics calculations,[14] the α and *β* rotamers of **VP** are nearly isoenergetic and only 1.5−2 kcal/mol more stable than the **p** structure with a 90° dihedral angle between the vinyl and pyridine planes. DFT calculations also predict that the α and *β* rotamers of **VP** are nearly isoenergetic but 6 kcal/mol lower in energy than the **p** structure.

Therefore, at room temperature, **VP** exists probably as a mixture of α and *β* rotamers in equilibrium. The formation of ylides *β* may be favored by the steric interaction between the vinyl and the approaching carbene, but this steric interaction should be small if the approach occurs as indicated on Scheme 3. In fact, the relative amounts of α and *β* ylides formed initially are not important because in the ylide the vinyl group is able to explore the α and *β* positions rapidly. This is indicated by

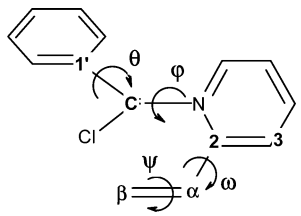

Figure 5. Numbering and lettering of atoms and rotation angles involved in the discussion of the structure of ylide rotamers.

TABLE 2: Calculated ΔH_f[a] for the Rotamers of 2-Vinylpyridine, VP-α and VP-*β*, and for the Transition State between Them, VP-p

relative ΔH_f [b]	VP-α	VP-p	VP-*β*
MOPAC + PM3	+0.22	+ 1.37	0
MOPAC + AM1	0	+1.85	+1.80
DFT	0	+6.0	+0.87

[a] Relative values. [b] In kcal/mol, calculated using the method indicated in the first column.

TABLE 3: Calculated ΔH_f for the α and *β* Rotamers of the 2-Vinylpyridinium Ylide of Phenylchlorocarbene and for the Transition State between Them, P

ΔH_f [a]	$\omega^b = 45°$ (α)	$\omega^b = 90°$ (**P**)	$\omega^b = 175°$ (*β*)
ylide type 1	91.1	89.4	90.2
ylide type 2	92.0	90.5	90.0

[a] In kcal/mol, calculated using MOPAC with PM3 parameters. [b] Locked angle.

TABLE 4: Calculated ΔH_f for Rotamers 1 and 2 of the 2-Vinylpyridinium Ylide of Phenylchlorocarbene and for the Transition State between Them, 3

ΔH_f [a]	ylide **1**	ylide **3**	ylide **2**
$\omega = 55°$ (α)	92.75	103.38	93.36
$\omega = 160°$ (*β*)	90.28	100.92	91.28

[a] In kcal/mol, calculated using MOPAC with PM3 parameters.

(1) the fact that there is no long-lived (ms) ylide absorption, although the cyclization of *β*-type ylides is impossible because the *β* vinylic carbon is too far away from the carbene center;

(2) calculations of the ΔH_f for ylide structures α**1**, α**2**, *β***1**, and *β***2** as well as those of structures **P1** and **P2** where the ω angle is set to 90°. The energies calculated for these structures are all within the 89.4−92.0 kcal/mol range of values.

Thus, α and *β* rotamers of the ylide species must be in fast equilibrium, whereas this cannot be the case for the rotamers detected experimentally because their τ_{growth} and τ_{decay} differ by a factor of 3. Therefore, the observed phenomenon is not related to rotamerism of type α ↔ *β*.

Rotamerism 1 ↔ 2. The calculated values of ΔH_f for ylide structures α**3** and *β***3** with a φ angle set to 90°, assumed to represent the transition states between ylides α**1** and α**2** and ylides *β***1** and *β***2** respectively, are 9.5 to 10 kcal/mol higher than those calculated for structures α**1**, α**2**, *β***1**, and *β***2**.

This value is in good agreement with the estimate of the activation energy for the interconversion of ylides $\mathbf{Y_1}$ and $\mathbf{Y_2}$, around 10 kcal/mol, obtained from the order of magnitude of rate constants k_{12} and k_{21} resulting from the kinetic analysis of the system. Therefore, the observed species $\mathbf{Y_1}$ and $\mathbf{Y_2}$ must be assigned to structures **1** and **2**, each one being a mixture of α and *β* geometries in fast equilibrium. However, $\mathbf{Y_1}$ has not yet been identified as being either structure **1** or structure **2**.

Attempts to Identify the Observed Species. We first tried to identify red-absorbing ylide $\mathbf{Y_2}$ as either structure **1** or structure **2** by using the fact that its rate of cyclization is larger than that for the other and thus the *Ea* barrier for its cyclization should be lower. The energy profile of the reactions ylide α**1** → DHI(1) and ylide α**2** → DHI(2) shown in Figure 6 was calculated as follows. Starting from structures α**1** and α**2** where the distance between the carbene center and the terminal vinylic carbon, *d*, is set to 4 Å, ΔH_f was calculated for decreasing values of *d* using MOPAC with PM3 parameters. Transition states for the cyclization appear for $d = 2.3$ Å with $\Delta H_f = 115$ kcal/mol when starting from ylide α**1** and for $d = 2.25$ Å with $\Delta H_f = 118.5$ kcal/mol when starting from ylide α**2**. The calculated

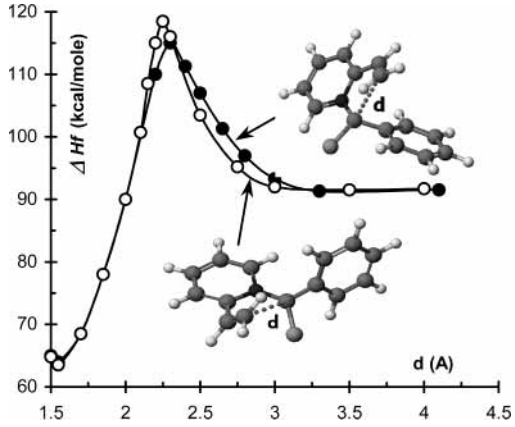

Figure 6. Calculation of the activation-energy barrier for the cyclization of ylides α**1** and α**2** using the MOPAC module of CAChe 3.2 with PM3 parameters.

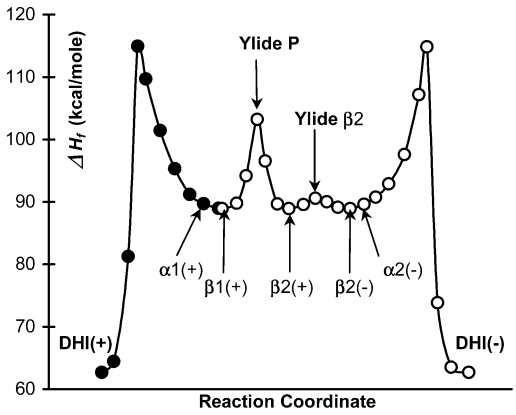

Figure 7. Energy profile, as calculated with AMPAC 7.2, for the cyclization pathways: (●−●) between ylide *β***1** and **DHI** of the same stereochemistry and (○−○) between ylide *β***1** and **DHI** with a change from type **1** to type **2** and a change in the stereochemistry from **2**(+) to **2**(−).

activation-energy barrier is thus around 24 kcal/mol in the first case and 27 kcal/mol in the second. These values are too large because considering the value of cyclization rate constants k_3 and k_4 the real value of *Ea* must be around 10 kcal/mol or even less when taking into account the entropy factor. The same calculations with AM1 parameters gave similar results: the *Ea* values calculated for the cyclization of ylides α**1** and α**2** are both around 20 kcal/mol, still too large and not significantly different.

The energy profile of the cyclization reaction path shown in Figure 7 was calculated using AMPAC 7.2[15] with PM3 parameters. It gives a complete view of the reaction scheme with rotations along the φ and ω angles. Again the energy barrier to the cyclization reaction (∼25 kcal/mol) is overestimated, but it is the same, within less than 1 kcal/mol, for the two rotamers. Therefore, the structures of $\mathbf{Y_1}$ and $\mathbf{Y_2}$ cannot be determined in this manner. This is not really unexpected because the rates of cyclization differ only by a factor of 5, which corresponds to a 1 kcal/mol difference between the *Ea* values.

The UV−vis absorption spectra of $\mathbf{Y_1}$ and $\mathbf{Y_2}$ being largely different, we calculated these absorption spectra for structures **1** and **2** with the hope that one of them would be significantly red shifted and could be assigned to $\mathbf{Y_2}$. The calculated absorption spectra are extremely sensitive to changes in the value of the θ angle, whereas the calculated ΔH_f is not. As shown in Figure 8, the λ_{max} of the absorption spectrum calculated for structure α**1** changes from 440 to 570 nm when θ decreases from 65 to 35°, whereas the ΔH_f values are equal within 1% or less, around 91 kcal/mol. Calculations of structure α**2** gave similar results: when θ decreases from 70 to 30°, λ_{max} increases from 420 to 550 nm, and the ΔH_f values are all in the range of 92.4−93.3 kcal/mol. The same tendency is obtained for structures *β***1** and *β***2**, calculated to be 1 or 2 kcal/mol more stable than the corresponding α rotamers, with λ_{max} in the range of 440−530 nm. These calculations indicate that the 100-nm difference between the λ_{max} of the observed species, $\mathbf{Y_1}$ and $\mathbf{Y_2}$, can be explained by the value of the θ angle, most probably around 30−35° for the red-absorbing species and 60−70° for the other. However, it is impossible to assign one of the observed species to either structure **1** or structure **2** because the ΔH_f values calculated for structure **1** with $\theta = 65°$ and structure **2** with $\theta = 30°$ (or inversely **1** with $\theta = 35°$ and **2** with $\theta = 60°$) are about the same.

About Stereochemistry. Although in the present case the rapid elimination of HCl does not allow an experimental study of the stereochemistry of the cyclization product, **DHI**, two stereoisomers of this product may be formed, and one may intuitively relate their formation to the two ylide rotamers ***1*** and ***2***. This intuition is incorrect!

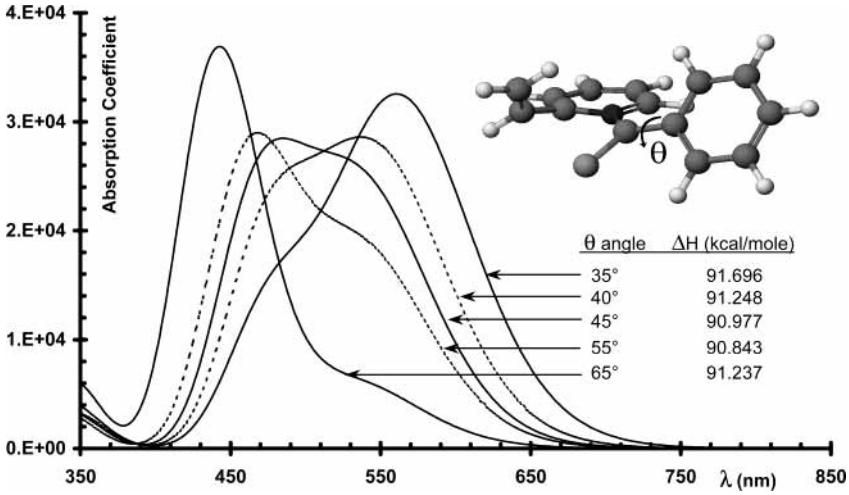

Figure 8. Absorption spectrum of ylide α**2** calculated using ZINDO for several values of the θ angle after optimization of the geometry by MOPAC with PM3 parameters

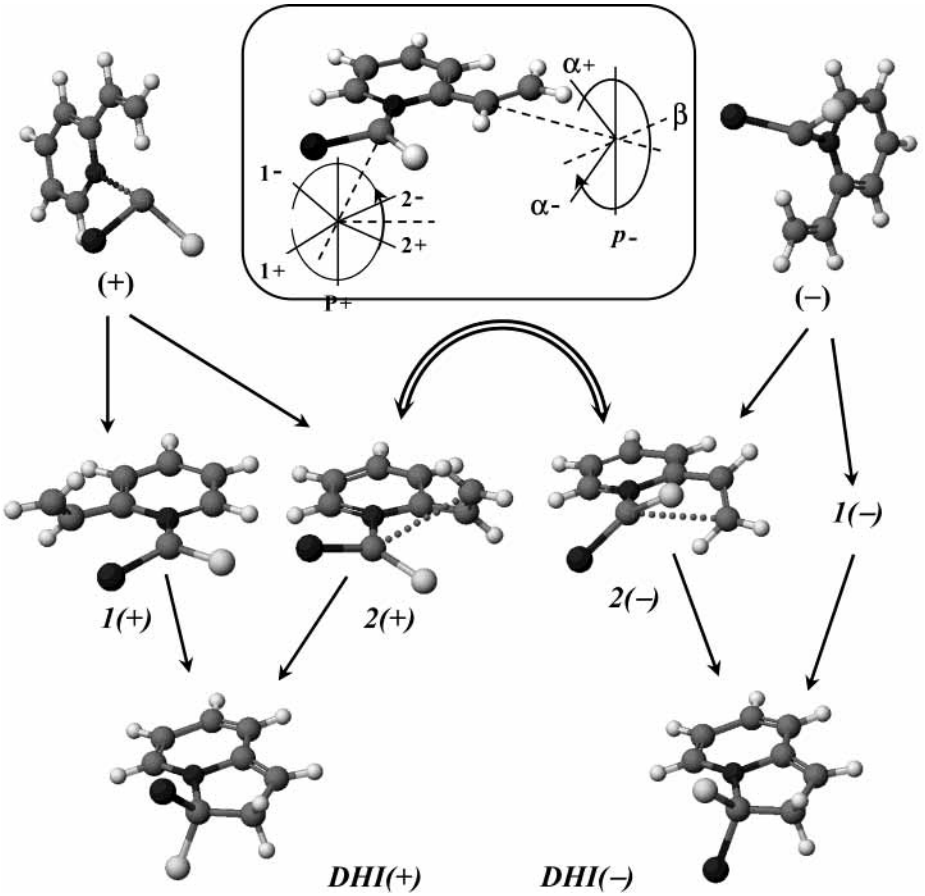

Figure 9. Stereochemistry of the system. For simplification, phenylchlorocarbene was changed to bromochlorocarbene (Br: dark gray, Cl: light gray). Dotted lines indicate the bond to be formed. Interconversion between the (+) and (−) ylides (e.g., from **2**(+) to **2**(−) with the vinyl passing from above to below the carbene plane) is possible by the concerted rotations of the carbene and vinyl moieties indicated in the inset.

In fact, as shown in Figure 9, the cyclization of ***1*** and ***2*** gives the same stereoisomer of **DHI**. The stereochemistry of the product is defined by the structure of the transition state for ylide formation, (+) or (−) depending on the relative orientation of the carbene and **VP**, giving two pairs of ylide rotamers, ***1***(+)/***2***(+) and ***1***(−)/***2***(−).

Interconversion between the (+) and (−) ylide structures is impossible for the α rotamers shown in the figure because steric hindrance between the vinyl group and the carbene prevents the vinyl group from freely moving from above to below the carbene plane. By contrast, this interconversion is easily achieved via the β structure by the concerted rotations of the carbene and vinyl moieties indicated in the inset: the activation energy found on the energy profile of the reaction path calculated with AMPAC is less than 1 kcal/mol.

Conclusions

The two rotamers of the **PCC** ← **VP** ylide can be distinguished because they have different UV−vis absorption spectra and different kinetic behavior. The difference in kinetics may be observed despite the existence of a rotameric equilibrium because the rate constants for interconversion are not much larger than the rate constants for cyclization. The difference between the UV−vis absorption spectra of such similar species may seem exceedingly large, but calculations show that a decrease in the tilt angle, θ, of the phenyl from 60 to 40° can account for a 100-nm red shift of the λ_{max} without changing the enthalpy of formation by more than 1 kcal/mol. These calculations also indicate that the two rotamers are not differentiated by the rotation of the vinyl (rotamerism α ↔ β) but by the fact that the vinyl faces either the chlorine or the phenyl (rotamerism **1** ↔ **2**). The enthalpies of formation calculated for structures α**1**, α**2**, β**1**, and β**2** with various values of θ being the same within the accuracy of the semiempirical methods used, we can neither assign a precise structure to the observed species nor decide whether the difference in reactivity of one species is related to the distance between the bond-forming atoms or to the relative amounts of the α and β conformations.

Acknowledgment. R.B. gratefully acknowledges the contribution of his colleagues in the LPCM laboratory: Dr. M-T. Rayez, who performed the DFT calculations on the rotamerism of **VP**, and Pr Daniel Liotard, a member of the team working to develop and improve the AMPAC software, who calculated the energy profile of the cyclization reaction path.

References and Notes

(1) Oki, M.; Tsukahara, J.; Sonoda, Y.; Moriyama, K.; Nakamura, N. *Bull. Chem. Soc. Jpn.* **1988**, *61*, 4303−4308 and previous papers in the series. Oki, M.; Saito, R. *Chem. Lett.* **1981** 649−642. Takeda, N.; Tokitoh, N.; Okazaki, R. *Chem. Eur. J.* **1997**, *3*, 62−69.

(2) Mazzucato, U.; Momicchioli, F. *Chem. Rev.* **1991**, *91*, 1679−1719. Spalletti, A.; Bartocci, G. *Phys. Chem. Chem. Phys.* **1999**, *1*, 5623−5632.

(3) For an example of such an observation, see Belin, C.; Béarnais-Barbry, S.; Bonneau, R. *J. Photochem. Photobiol.*, **2001**, *139*, 111−124.

(4) Liu, M. T. H.; Romashin, Y. N.; Bonneau, R. *Int. J. Chem Kinet.* **1994**, *26*, 1179−1184.

(5) Graham, W. H. *J. Am. Chem. Soc.* **1965**, *87*, 4396−4398.

(6) Jackson, J. E.; Soundararajan, N.; Platz, M. S.; Liu, M. T. H. *J. Am. Chem. Soc.* **1988**, *110*, 5595−5596.

(7) Bonneau, R.; Collado, D.; Liu, M. T. H. *J. Photochem. Photobiol., A* **2003**, *161*, 43−50.

(8) Naito, I.; Uryu, T.; Sasaki, H.; Ishikawa, T.; Kobayashi, S.; Kamata, I.; Oku, A. *J. Photochem. Photobiol., A* **2001**, *140*, 33−38. The rates measured for the carbene decay and the ylide formation are different (182 and 138 ns, respectively, when [**VP**] = 18 mM according to their Figure 3), and from their Figure 2, the λ_{max} of the time-resolved ylide absorption spectrum shifts from ~600 to 540 nm as the delay after excitation increases from 0.1 to 2.4 μs

(9) Malinowski, E. R. *Factor Analysis in Chemistry*, 2nd ed. Wiley & Sons: New York, 1991.

(10) Assuming no equilibration between the rotamers, the faster decay of rotamer $\alpha 2$ would decrease its apparent τ_{growth} a little bit, by 10−15%, but could not decrease it by a factor of 3.

(11) This gives k_1 and $k_2 \approx 7 \times 10^7$ s^{-1} because [**VP**] ≈ 10 mM.

(12) The value of the ratio k_1/k_2 mainly affects the ratio between the maxima of the calculated concentrations of ylides **1** and **2**. It was set equal to 1.33 in this simulation because the absorption coefficients the two species, ϵ_1 and ϵ_2, were assumed to be the same, but it would be unity if ϵ_1 was larger than ϵ_2 by 35%.

(13) With $k_{21}/k_{12} = 10$, one gets $\Delta G \approx 1.3$ kcal/mol, and assuming that the frequency factor for the interconversion of rotamers is around 5×10^{12} s^{-1}, the value of k_{21} yields $\Delta E_a \approx 10.5$ kcal/mol.

(14) *MOPAC* with AM1 and PM3. Commercial package *CAChe 3.2* from Oxford Molecular Ltd., 1999.

(15) *AMPAC.7.2* from Semichem Inc., Shawnee, KS, 2003.